arXiv:1603.00363v3 [cond-mat.mes-hall] 16 Dec 2016

Enhancement of crossed Andreev reflection in a superconducting ladder connected to normal metal leads

Abhiram Soori[1] and Subroto Mukerjee[2]

[1] *International Centre for Theoretical Sciences (TIFR), 151, Shivakote, Bengaluru 560089, India*
[2] *Department of Physics, Indian Institute of Science, Bengaluru 560012, India*

(Dated: December 19, 2016)

Crossed Andreev reflection (cAR) is a scattering process that happens in a quantum transport set-up consisting of two normal metals (NM) attached to a superconductor (SC), where an electron incident from one NM results in a hole emerging in the other. Typically, an electron tunnelling through the superconductor from one NM to the other (ET) competes with cAR and masks the signature of cAR in the conductance spectrum. We propose a novel scheme to enhance cAR, in which SC part of the NM-SC-NM is side-coupled to another SC having a different SC phase to form a Josephson junction in the transverse direction. At strong enough coupling and adequate phase difference, one can smoothly traverse between highly ET-dominant to highly cAR-dominant transport regimes by tuning chemical potential, due to the appearance of subgap Andreev states that are extended in the longitudinal direction. We also discuss connections to realistic systems.

Introduction : Andreev reflection (AR) is the scattering process by which a current flows across the interface of a normal metal (NM) and a superconductor (SC) when an external bias across the interface is applied in the subgap regime. The Cooper-pair current in the superconductor draws equal contributions from the electron and hole channels of the normal metal. This phenomenon, first discovered by Andreev [1] has been extensively studied theoretically and experimentally for several decades [2–4]. AR has played an important role in observing transport signatures of exotic Majorana fermions in mesoscopic systems [4]. In addition, recent advances in cold-atomic systems promise new testbeds where theoretical findings [5, 6] related to Andreev reflection can be demonstrated experimentally [7]. Crossed Andreev reflection (cAR) is a phenomenon closely related to AR which happens in a system consisting of two normal metals attached to a superconductor [8–21]. An electron incident on the SC from the first normal metal (NM1) gets absorbed into the SC as a Cooper-pair, absorbing the second electron of the Cooper-pair from the second normal metal (NM2), resulting in a hole current in the second normal metal. The phenomenon of cAR is closely related to the production of non-locally entangled electrons by splitting Cooper pairs from the SC, the detection and enhancement of which has seen lot of theoretical [22] and experimental interest [23, 24]. However, cAR is accompanied by electron tunneling (ET) where the electron from the NM1 tunnels into the NM2 as an electron. cAR is typically masked in simple NM-SC-NM systems due to a dominant ET [10]. A negative differential transconductance between NM1 and NM2 is a definite signature of cAR.

In this paper, we propose a novel scheme to enhance cAR, which is different from other existing proposals [9, 11–18, 25], and demonstrate with a simple theoretical model that cAR enhancement can be much higher. Of the two existing proposals that have been experimentally demonstrated, the first method is to introduce barriers at the NM-SC junctions of an NM-SC-NM set-up [16, 20], while the second one is to employ two ferromagnets (FM) in anti-parallel configuration instead of the NM's [17–19] that will suppress ET and AR and thereby allow cAR to dominate. cAR is enhanced in the former method when the momentum scale characterizing the barrier is at least as large as the Fermi-momentum, though the enhanced cAR currents are too small [25]. In addition, there are several other proposals such as: (i) to employ quantum spin Hall insulators connected to SC and spatially separate ET and cAR channels based on the spin-momentum locking of the edge states [11], (ii) to drive a steady Cooper pair current in the SC such that the SC phase modulates and thus enhance cAR [12], (iii) to substitute NM and SC parts of the setup with exotic materials such as graphene, silicene, topological insulators and topological superconductors [13, 14], (iv) coupling to external electromagnetic modes [15], which have not yet seen experimental implementation. We propose to modify the NM-SC-NM setup by side-coupling the SC part with another SC (which has a SC phase differing by ϕ but has the same magnitude of the SC pair potential) as shown in Fig. 1(a). We call the two coupled SC's together as "SC ladder". We show that an adequate SC phase difference between two legs of the ladder accompanied by a sufficiently strong coupling between the two legs of the SC ladder leads to subgap Andreev states which can enhance cAR. This is the central result of our work.

Calculation : Introducing the hole annihilation operators $d_{s,\lambda}(x) = c^{\dagger}_{\bar{s},\lambda}(x)$, the Hamiltonian for the ladder region ($0 \leq x \leq a$) can be written as:

$$H = \sum_{\lambda,s}\Bigg[\Psi^{\dagger}_{s,\lambda}(x)\Big\{\Big(\frac{-\hbar^2}{2m}\frac{\partial^2}{\partial x^2}-\mu\Big)\tau_z + \Delta(\cos\phi_\lambda\tau_x + \sin\phi_\lambda\tau_y)\Big\}\Psi_{s,\lambda}(x) + g\ \Psi^{\dagger}_{s,\lambda}(x)\tau_z\Psi_{s,\bar{\lambda}}(x)\Bigg], \quad (1)$$

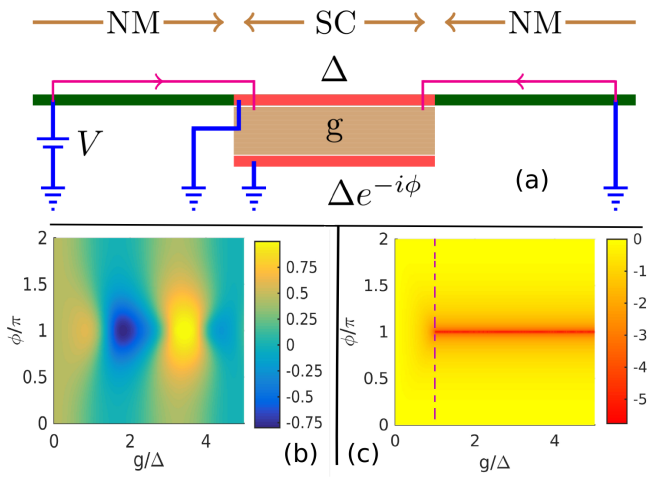

FIG. 1: (a) A schematic diagram of the set-up. Thick red lines in the middle are two SC-channels, coupled to each other by a strength g-highlighted by a brown region in between. A voltage bias V is applied from left NM while SC-ladder and the right NM are grounded, as shown by the blue lines. Thin lines with arrow show the current directions when cAR dominates over ET. (b) The zero bias transconductance G_{RL} in units of $2e^2/h$. (c) The logarithm of the gap in the dispersion of the ladder region [Eq. (2)] in units of Δ; the vertical dashed line points to the line $g/\Delta = 1$. Parameters: $\mu = 10\Delta$, $a = 6\hbar/\sqrt{2m\Delta}$.

where (i) $s = \uparrow, \downarrow$ and $\lambda = 1, 2$ are spin and wire indices respectively, (ii) $\bar{s}/\bar{\lambda}$ takes the value of the label index different from s/λ, and (iii) $\Psi_{s,\lambda}(x) = [\sigma_s c_{s,\lambda}(x),\ d_{s,\lambda}(x)]^T$, where $\sigma_{\uparrow/\downarrow} = \pm 1$. The dispersion for this Hamiltonian is:

$$E = \pm\sqrt{\epsilon_k^2 + g^2 + \Delta^2 \pm 2g\sqrt{\epsilon_k^2 + \Delta^2 \sin^2\left[(\phi_1 - \phi_2)/2\right]}}, \tag{2}$$

where $\epsilon_k = (\hbar^2 k^2/2m - \mu)$ and $\hbar k$ is the momentum. Each of these bands is doubly degenerate due to spin ($s = \uparrow, \downarrow$). The Hamiltonians for the NM regions on the left ($x < 0$) and right ($x > a$) are given by $H = \sum_s c_s^\dagger(x)[\hbar^2 k^2/2m - \mu]c_s(x)$. Here onwards, we shall leave out the spin index s. A factor of 2 to account for spin degeneracy will multiply the conductances in the final result. The SC phases ϕ_λ on the two legs ($\lambda = 1, 2$) of the SC ladder can be chosen to be $\phi_1 = 0$, and $\phi_2 = -\phi$, without loss of generality so that $(\phi_1 - \phi_2) = \phi$.

Solution to the Hamiltonian will be a two-spinor ψ in the NM-regions (two components represent the electron- and hole- channels) and a four-spinor $[\psi^T,\ \chi^T]^T$ in the ladder region (two more components represent the second leg of the ladder), where the spinors ψ and χ have the form: $\psi(x) = [\psi_e(x),\ \psi_h(x)]^T$ for $-\infty < x < \infty$ and $\chi(x) = [\chi_e(x),\ \chi_h(x)]^T$ for $0 \le x \le a$. In the NM regions, the electrons and holes take momenta $\pm\hbar k_e$ and $\pm\hbar k_h$ respectively, where $k_{e/h} = \sqrt{2m(\mu \pm E)/\hbar^2}$ at a given energy E. The scattering wavefunction for an electron incident from left onto the ladder region at an energy E is given by:

$$\begin{aligned}
\psi_e(x) &= e^{ik_e x} + r_n e^{-ik_e x}, \quad \text{for} \quad x \le 0, \\
&= t_n e^{ik_e x}, \quad \text{for} \quad x \ge a, \\
\psi_h(x) &= r_a e^{ik_h x}, \quad \text{for} \quad x \le 0, \\
&= t_a e^{-ik_h x}, \quad \text{for} \quad x \ge a, \\
\psi(x) &= \sum_{\sigma,\nu,p} s_{\sigma,\nu,p} e^{i\sigma k_{\nu,p} x}[\psi_{e,\nu,p}\ ,\ \psi_{h,\nu,p}]^T \text{ and} \\
\chi(x) &= \sum_{\sigma,\nu,p} s_{\sigma,\nu,p} e^{i\sigma k_{\nu,p} x}[\chi_{e,\nu,p}\ ,\ \chi_{h,\nu,p}]^T, \\
&\quad \text{for} \quad 0 \le x \le a.
\end{aligned} \tag{3}$$

In the ladder region, the momenta $\sigma\hbar k_{\nu,p}$ at energy E denoted by the indices σ, ν, p are obtained by inverting the dispersion relation Eq.(2): $\hbar k_{\nu,p} = \sqrt{2m(\sigma_p \epsilon_{k,\nu} + \mu)}$, where $\epsilon_{k,\nu} = \sqrt{E^2 + g^2 - \Delta^2 + 2g\nu\sqrt{E^2 - \Delta^2\cos^2(\phi/2)}}$, and the index $\sigma = \pm 1$ denotes whether the mode is right/left-mover, the index $\nu = \pm 1$ refers to the anti-bonding/bonding bands formed due to hybridization between the two legs ($\lambda = 1, 2$) of the ladder and $p = e, h$ refer to electron, hole -like bands for which $\sigma_{e/h} = \pm 1$.

From the boundary conditions (BC's) described by Carreau et. al [26] for a general one dimensional system, we choose the BC that is physically relevant to our system [25]:

$$\begin{aligned}
&\psi(x_0^+) = \psi(x_0^-)\ , \quad \partial_x\psi(x)|_{x=x_0^+} = \partial_x\psi(x)|_{x=x_0^-}\ , \\
&\partial_x\chi(x)|_{x=x_0} = 0 \quad \text{for } x_0 = 0,\ a.
\end{aligned} \tag{4}$$

Both the NMs are connected to only one leg ($\lambda = 1$) of the SC ladder as shown in Fig. 1(a). The junction is modeled to be transparent since we are interested in enhancing cAR - a scattering process which involves both the NMs. We have calculated the scattering amplitudes numerically for a diverse set of relevant parameters by employing the BC- eq.(4) in the wavefunction given by Eq.(3). Using these scattering amplitudes, the transconductance has been calculated. The transconductance is the physical quantity of interest since it can be experimentally measured.

The set-up under investigation is essentially a three terminal set-up. While the NM regions on left and right (extending to $x \to \mp\infty$) form two terminals, the SC ladder in the middle (maintained at a fixed chemical potential μ) acts as a reservoir for the charge current since charge current is not conserved in the SC region. We are interested in calculating the differential transconductance $G_{RL}(V) := dI_R(V)/dV$ - where $dI_R(V)$ is the change in current in the right NM when the Fermi energy of the left NM is changed from eV to $e(V + dV)$, keeping the Fermi energies of the ladder region and right

NM at zero (here, e is the electronic charge and V is the voltage). Using Landauer-Büttiker formalism [27], the differential transconductance in such a transport set-up at a bias voltage V can be written as:

$$G_{RL}(V) = \frac{2e^2}{h}\Big(|t_n|^2 - |t_a|^2\sqrt{(\mu - eV)/(\mu + eV)}\Big) \quad (5)$$

It is easy to see from Eq.(5) that the contributions of ET and cAR to the current on the right NM are positive and negative respectively. Hence, a negative G_{RL} is a clear signature of cAR enhanced over ET while a positive G_{RL} implies the dominance of ET over cAR.

Results : (1) We look at the zero-bias transconductance $G_{RL}|_{V=0}$ as a function of the parameters ϕ and g as shown in Fig. 1 (b) and understand it in terms of the dispersion of the ladder region given by Eq.(2). Fig. 1 (c) is a contour-plot of the logarithm of the gap in units of Δ (i.e., $\log[E_g/\Delta]$). The gap closes on the line: $g/\Delta \geq 1$, $\phi = \pi$. And, cAR is enhanced as g/Δ crosses 1 from left to right and this enhancement is prominent around $0.7\pi < \phi < 1.3\pi$ and $1.4\Delta < g < 2.2\Delta$. Further, as g/Δ crosses a value of 3, ET is enhanced to a value as high as $\sim 0.75 \cdot 2e^2/h$. This indicates that enhancement of cAR and ET to such high values is related to closing of the gap.

(2) We fix $\phi = \pi$ and see how the subgap conductance spectrum changes as the coupling strength g is changed. This is contrasted with the dispersion of the ladder region, the topology of which changes when g/Δ is on either side of 1. In Fig. 2 (a-c), the dispersion of the SC ladder, and in Fig. 2 (d-f), the conductance spectrum for $g/\Delta = 0.5,\ 1.0,\ 1.5$ have been plotted. As g/Δ crosses over from 0.5 to 1.5, through 1.0, the conductance spectrum shifts smoothly from being in the positive-half to being in the negative-half of the ordinate, which is a clear signature of enhanced cAR as indicated by the green dotted lines. And this is accompanied by appearence of subgap Andreev states in the SC ladder.

(3) Now, we explore the dependence of the conductance spectrum in the bias window ($|eV| \leq \Delta$) to the SC phase difference ϕ and the chemical potential μ. Fig. 2 (g-h) show contour plots of G_{RL} as function of (eV, ϕ) for $g = 0.5\Delta$ [2(g)] and $g = 1.5\Delta$ [2(h)]. One can see that cAR is enhanced significantly for the case $g = 1.5\Delta$ throughout in the bias window $(-\Delta, \Delta)$, and the value of ϕ at which cAR is enhanced the most depends on the value of the bias eV. Though cAR is enhanced in the case of $g = 0.5\Delta$, this happens in very narrow regions of the $eV - \phi$ plane, and it is worth noting that the enhancement of cAR for $g = 0.5\Delta$ happens for values of ϕ far away from zero or 2π.

(4) Fig. 2 (i-j) show contour plots of G_{RL} as a function of (eV, μ) for $g = 0.5\Delta$ [2(i)] and $g = 1.5\Delta$ [2(j)]. For these two cases, $\phi = \pi$. It is apparent from the contour-plots that the enhancement of cAR is prominent in the case of $g = 1.5\Delta$ compared to the case of $g = 0.5\Delta$. For

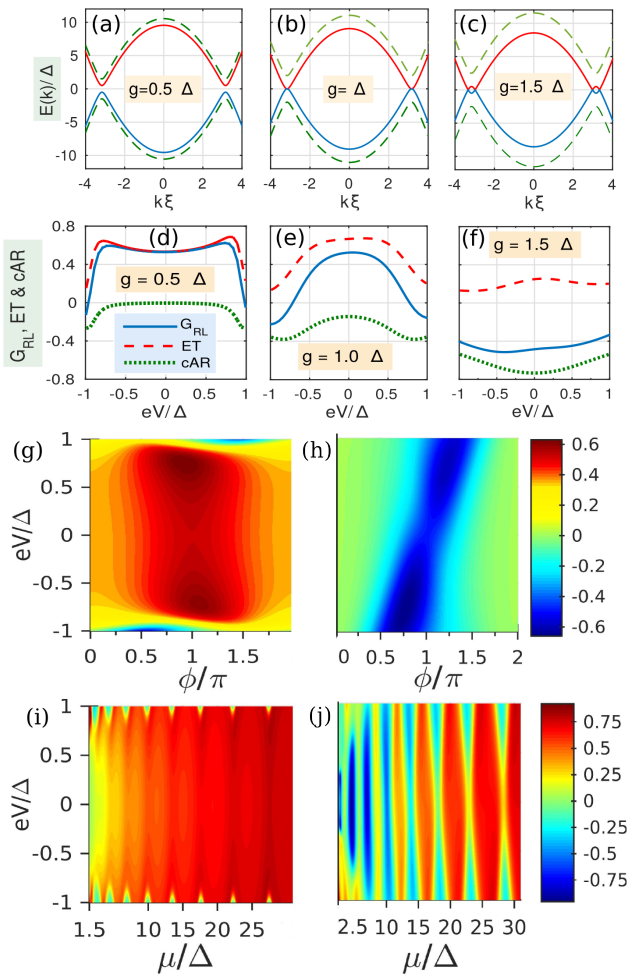

FIG. 2: (a-c): Dispersion of the SC ladder, (d-f): transconductance G_{RL}, contributions to it from ET and cAR for $\phi = \pi$, $\mu = 10\Delta$. (g-j): Contour plots of G_{RL}. For (g, i), $g = 0.5\Delta$. For (h, j), $g = 1.5\Delta$. For (d-j), $a = 6\hbar/\sqrt{2m\Delta}$. For (g, h), $\mu = 10\Delta$. For (i, j), $\phi = \pi$. G_{RL} is units of $2e^2/h$.

$g = 1.5\Delta$, cAR is enhanced throughout the bias window around certain values of μ, but for $g = 0.5\Delta$, a poor cAR enhancement can be found in very small regions near $eV = \pm\Delta$. Further, the enhancement of cAR occurs at a series of μ_i's. Also, the enhancement of cAR around the μ_i's becomes less prominent with increasing μ_i.

Mechanism : The above results point us to the following mechanism for enhancement of cAR. A nonzero phase-difference ϕ and a non-zero coupling g between two legs of the ladder create plane-wave modes within the otherwise gapped dispersion of the ladder region as can be seen from Eq.(2). Equivalently, two out of four $k_{\nu,p}$'s become real valued at energies: $|E| < \Delta$. These planewave modes have nonzero components in both electron- and hole- sectors and we call them subgap Andreev states. Thus, the transconductance is due to Fabry-Pérot type interference between the subgap Andreev states in the ladder region that transmit either an electron or a hole into right NM,

the probabilities of which can be tuned by changing a parameter that changes the dispersion and the spinor structure of the modes in the ladder region. The subgap Andreev states can be thought of as planewave modes formed by hybridisation of Andreev bound states, when a large number of Josephson junctions (each formed between two superconducting quantum dots) are coupled.

Since, chemical potential μ - sets the fundamental length-scale of the problem and affects the spinor structure of the BdG modes, changing μ smoothly, keeping the values of eV, ϕ ($\neq 0$) and g ($\neq 0$) fixed must show a smooth transition from maximally enhanced cAR to maximally enhanced ET. This can be seen in Fig. 2(j) and the recurrent enhancement of cAR and ET at a series of values of μ ($=\mu_i$) corresponds to a periodicity in k_i's (where $k_i = \sqrt{2m\mu_i/\hbar^2}$) [28], given by $(k_{i+1} - k_i)a \sim \pi$, reaffirming quantitatively our explanation that the cAR enhancement is due to Fabry-Pérot interference between the subgap Andreev states in the SC ladder. As can be seen from Fig. 1(c), having $\phi = \pi$ and $g > \Delta$ correspond to gap closing and hence the cAR enhancement is expected to be maximal for this choice of parameters, which is in agreement with the results highlighted in Fig. 2 (d-j).

Discussion: We have primarily studied a one-dimensional superconductor side-coupled to another one dimensional superconductor. However, in reality, long-range superconducting order is not possible in purely one dimension. This limitation can be overcome by a proximate superconductor (pr-SC) in contact with the one-dimensional quantum wire. Also, the Fermi energy and chemical potential in the SC are assumed to be maintained at a particular value, which means that a steady state current flows into the SC and the SC is grounded via a grounding electrode.

We now discuss different systems that are closer to experimental setups in which our results can possibly be tested. To be able to maintain a SC phase difference ϕ between two legs of the ladder is an important task when it comes to experimental implementation. We point to the following directions to achieve this:

(1) One route is to pass a supercurrent in the transverse direction; a SC phase difference between two legs of the SC ladder is induced that is proportional to the transverse current [12].

(2) Another route is to use magnetic flux to mimic the Josephson phase difference as in SQUIDS [30]. Connecting two legs of the ladder through a loop and passing a magnetic flux through can induce a phase difference proportional to the flux (modulo flux quantum Φ_0) as discussed in ref. [31].

(3) π-junction materials, such as layered superconductors [32] have a non-zero SC phase difference naturally existing between the adjacent layers. Sandwiching such a layered SC between NM leads in such a way that each layer lies in the longitudinal direction can mimic the ladder structure proposed here. This will be a quasi-two-dimensional version of the setup we have proposed. We have performed transport calculations for such a two-dimensional version of the ladder geometry and we see that most of our results we obtained above remain the same qualitatively [25].

(4) The subgap Andreev states that appear in the ladder also appear in a closely related system- a *Josephson junction between two-dimensional superconductors*. To describe the system more precisely, let the regions: $(0 \leq y \leq \infty,\ 0 < x < a)$ and $(-\infty < y < 0,\ 0 < x < a)$ have SC phases Δ and $\Delta e^{-i\phi}$. Using appropriate BC at $y = 0$, the subgap states localised at the junction can be calculated [25]. We see that very similar to the ladder, a non-zero ϕ gives rise to subgap states which are BdG planewave modes along x-direction, but are localised in the y-direction around $y = 0$. These states can be used to enhance cAR if two NM metal leads are connected close to the Josephson junction.

The very fact that a phase difference is maintained between the two legs of the ladder, means that a Josephson current flows from one leg of the ladder to the other in the transverse direction. However, this current does not interfere with the quasiparticle current that is carried by the subgap Andreev states between the two NM leads. In a recent experiment [33] , it was demonstrated that a subgap Andreev bound state formed in a Josephson junction shows a subgap peak in conductance when connected to a NM. This is due to Andreev reflection and the current in the NM due to Andreev reflection does not interfere with the Josephson current that flows from one SC to the other. The existence of stabilised subgap modes is required to get enhanced cAR.

In a set-up where cAR is enhanced over ET and AR, if the bias is maintained across both the NM-SC junctions keeping the two NM's grounded, this is expected to result in a high-efficiency Cooper pair splitting (CPS). Once a considerable SC phase difference ($\pi/2 \lesssim \phi \lesssim 3\pi/2$) is maintained in the ladder, CPS can be enhanced by tuning either the chemical potential μ or the length a of the ladder region, in contrast to the already existing Cooper pair splitter [23, 24] which is based on Coulomb blockaded quantum dots, where two gate voltages need to tuned to a particular combination. In this spirit, our scheme may be less fragile to the parameters that need to be tuned to get CPS enhancement. Further, the conductances measured in the experiment reporting high efficiency CPS [24] suggest that the corresponding cAR enhanced transconductance values are much smaller in magnitude than the values that can be obtained theoretically in our set-up.

AS thanks Diptiman Sen, G Baskaran, Anindya Das, Oindrila Deb, Aviad Frydman, Efrat Shimshoni, Pascal Simon, Ady Stern, Manisha Thakurati, Aveek Bid, Hemanta Kundu and Alfredo Levy Yeyati for discussions. AS thanks Abhishek Dhar for support and encourage-

ment and *Infosys Excellence Grant for ICTS-TIFR, Bengaluru* for funding expenses to participate in *APS March meeting 2016*, where this work was presented. We thank Diptiman Sen for careful reading of the manuscript.

[1] A. F. Andreev, Sov. Phys. JETP 19, 1228 (1964).
[2] G. E. Blonder, M. Tinkham, and T. M. Klapwijk, Phys. Rev. B **25**, 4515 (1982).
[3] A. Kastalsky, A. W. Kleinsasser, L. H. Greene, R. Bhat, F. P. Milliken, and J. P. Harbison, Phys. Rev. Lett. **67**, 3026 (1991).
[4] V. Mourik, K. Zuo, S. M. Frolov, S. R. Plissard, E. P. A. M. Bakkers, and L. P. Kouwenhoven, Science **336**, 1003 (2012); S. M. Albrecht, A. P. Higginbotham, M. Madsen, F. Kuemmeth, T. S. Jespersen, J. Nygard, P. Krogstrup and C. M. Marcus, Nature 531, 206209 (2016).
[5] A. Soori and D. Sen, EPL, 93, 57007 (2010); A. Soori and D. Sen, Phys. Rev. B 84, 035422 (2011); I. Safi and H. J. Schulz, Phys. Rev. B 52, R17040 (1995).
[6] C. Chamon, M. Oshikawa, and I. Affleck, Phys. Rev. Lett. 91, 206403 (2003); M. Oshikawa, C. Chamon, and I. Affleck, J. Stat. Mech.: Theory Exp. 2006, P02008 (2006).
[7] T. Domanski, Phys. Rev. A 84, 023634 (2011); I. Zapata and F. Sols Phys. Rev. Lett. 102, 180405 (2009); A. J. Daley, P. Zoller, and B. Trauzettel, Phys. Rev. Lett. 100, 110404 (2008).
[8] J. M. Byers, M. E. Flatté, Phys. Rev. Lett. 74, 306 (1995).
[9] G. Deutscher and D. Feinberg, App. Phys. Lett. 76, 487 (2000); G. Falci, D. Feinberg and F. W. J. Hekking, EPL 54, 255 (2001).
[10] R. Mélin, F. S. Bergeret, and A. Levy Yeyati, Phys. Rev. B 79, 104518 (2009).
[11] R. W. Reinthaler, P. Recher, and E. M. Hankiewicz, Phys. Rev. Lett. 110, 226802 (2013).
[12] Wei Chen, D. N. Shi and D. Y. Xing, Scientific Reports 5, 7607 (2015).
[13] S. Gómez, P. Burset, W. J. Herrera, and A. Levy Yeyati, Phys. Rev. B 85, 115411 (2012); J. Linder and T. Yokoyama, Phys. Rev. B 89, 020504(R) (2014); J. Linder, M. Zareyan, and A. Sudbo, Phys. Rev. B 80, 014513 (2009); J. Wang, L. Hao, and K. S. Chan, Phys. Rev. B 91, 085415 (2015); F. Crépin, H. Hettmansperger, P. Recher, and B. Trauzettel, Phys. Rev. B 87, 195440 (2013).
[14] J. J. He, J. Wu, T-P Choy, X-J Liu, Y. Tanaka and K. T. Law, Nat Commun. 5, 3232 (2014).
[15] A. Levy Yeyati, F. S. Bergeret, A. Martin-Rodero and T. M. Klapwijk, Nature Physics 3, 455 (2007).
[16] N. M. Chtchelkatchev, JETP Lett. 78, 230 - 235 (2003).
[17] R. Mélin and D. Feinberg, Phys. Rev. B 70, 174509 (2004), M. Božović and Z. Radović, Phys. Rev. B 66, 134524 (2002), Z. C. Dong, R. Shen, Z. M. Zheng, D. Y. Xing, and Z. D. Wang, Phys Rev B 67, 134515 (2003).
[18] T. Yamashita, S. Takahashi, and S. Maekawa, Phys. Rev B 68, 174504 (2003).
[19] D. Beckmann, H. B. Weber, and H. v. Löhneysen, Phys. Rev. Lett. 93, 197003 (2004); D. Beckmann, and H. v. Löhneysen, AIP Conf. Proc. 850, 875 (2006).
[20] S. Russo, M. Kroug, T. M. Klapwijk, and A. F. Morpurgo, Phys. Rev. Lett. 95, 027002 (2005).
[21] K. Sun, N. Shah, and S. Vishveshwara, Phys. Rev. B 87, 054509 (2013).
[22] P. Recher, E. V. Sukhorukov, and D. Loss, Phys Rev B 63, 165314 (2001); C. Bena, S. Vishveshwara, L. Balents, and M. P. A. Fisher, Phys. Rev. Lett. 89, 037901 (2002).
[23] A. Das, Y. Ronen, M. Heiblum, D. Mahalu, A. V. Kretinin, Nat Commun 3, 1165 (2012).
[24] J. Schindele, A. Baumgartner, and C. Schönenberger, Phys. Rev. Lett. 109, 157002 (2012).
[25] See supplementary information for further discussion.
[26] M. Carreau, E. Farhi, and S. Gutmann, Phys. Rev. D 42, 1194 (1990).
[27] R. Landauer, IBM J. Res. Dev. 1, 223 (1957), and Philos. Mag. 21, 863 (1970); M. Büttiker, Y. Imry, R. Landauer, and S. Pinhas, Phys. Rev. B 31, 6207 (1985); M. Büttiker, Phys. Rev. Lett. 57, 1761 (1986); S. Datta, *Electronic Transport in Mesoscopic Systems* (Cambridge University Press, Cambridge, 1995).
[28] Though exact expression for k_i needs to be obtained by inverting the dispersion Eq.(2) as explained in the text after Eq.(3), the approximation $k_i = \sqrt{2m\mu_i/\hbar^2}$ is valid when $\mu \gg g > \Delta \geq |E|$.
[29] A. Soori, S. Das, and S. Rao, Phys. Rev. B 86, 125312 (2012).
[30] M. Tinkham, Introduction to Superconductivity (McGraw-Hill, New York, 1975), Chapter 6.
[31] A. Keselman, L. Fu, A. Stern, and E. Berg, Phys. Rev. Lett. 111, 116402 (2013)
[32] D. Z. Liu, K. Levin, and J. Maly, Phys. Rev. B 51, 8680(R) (1995).
[33] J-D. Pillet, C. H. L. Quay, P. Morfin, C. Bena, A. Levy Yeyati and P. Joyez, Nature Phys 06, 965 (2010).

SUPPLEMENTARY INFORMATION

Here, we discuss (i) the boundary condition (BC) employed, (ii) cAR enhancement in simpler set-up consisting of just two normal metals (NM) and a superconductor (SC), (iii) a Josephson junction between two-dimensional superconductors, and (iv) transport in a layered SC with a phase difference.

Boundary conditions used in our calculations

In this part, we shall discuss details of the boundary condition (BC) used in the main paper for the SC ladder connected to NM leads. The NM-SC junction generically has a barrier to the electron tunneling which limits the electron transmission. The BC at NM-SC interface is described by continuity of the wave-function and a discontinuity of the derivative [3]. The latter is the same as having a delta-function barrier potential on the NM side of the NM-SC junction, infinitesimally close to the junction. Since we are interested in enhancing cAR over ET, we shall set the barrier strengths to zero to make the NM-SC junctions fully transparent. In other words, both the wavefunction and its derivative at the NM-SC interface are continuous. But this fixes the BC only for one leg of the ladder. The BC for the other leg is given by a probability current conserving BC at the ends of the ladder (i.e., $x = 0,\ a$). Such a BC that describes the lower leg of the ladder has four-parameters in general as explored for a 'particle in box' by Carreau et. al [4]. The NM-SC interfaces at $x = 0,\ a$ are not connected by any direct hopping as in the case of a periodic BC. This reduces the BC to have just two parameters: $(q_{2,x_0} + \partial_x)\Psi_2(x)|_{x=x_0} = 0$, where q_{2,x_0} is a real-valued parameter with dimensions of inverse length that describes the BC at x_0. The limit $q_{x0} \to \infty$ implies that the wavefunction is zero at $x = x_0$, while the limit $q_{x0} \to 0$ implies that the first derivative of the wavefunction is zero at x_0, allowing the wavefunction to have a non-zero probability density at x_0. The latter limit qualitatively corresponds to a lattice model of a SC ladder where the last site of the second leg can have a finite probability density. Hence, we have further chosen $q_{x_0} = 0$ for both $x_0 = 0$ and $x_0 = a$, though a particular choice of the BC does not affect the results qualitatively. Below are the BC's written down in the form of equations:

$$\psi(x_0^+) = \psi(x_0^-)\ , \quad \partial_x\psi(x)|_{x=x_0^+} = \partial_x\psi(x)|_{x=x_0^-}\ ,$$
$$\partial_x\chi(x)|_{x=x_0} = 0 \quad \text{for } x_0 = 0,\ a. \tag{6}$$

NM-SC-NM with barriers

Theoretical calculations by Chtchelkatchev [1] were done for a two-dimensional NM-SC-NM system with barriers at the junctions. We took the one-dimensional version of the NM-SC-NM set-up with barriers. We could reproduce their results qualitatively, i.e., cAR is enhanced by having barriers at the NM-SC interface. Fig. 3 summarises results of our calculations on single-channel SC connected to two NM leads with barriers of strength $q_0 = 5k_F$ (where $k_F = \sqrt{2m\mu/\hbar^2}$). The parameter q_0 enters the calculations through the BC:

$$\partial_x\psi(x)|_{x=\pm a+0} - \partial_x\psi(x)|_{x=\pm a-0} = q_0\ \psi(\pm a). \tag{7}$$

In certain narrow regions in the bias-k_Fa plane, cAR is enhanced. But the enhanced cAR contributions to the conductance are much smaller even in the theoretical calculations for a ballistic system ($0.15 \cdot 2e^2/h$ being the largest value obtained in this set-up to the maximum possible value of $2e^2/h$). The mechanism here is multiple back-and-forth reflections of the BdG quasiparticles in the SC due to the presence of barriers at the NS junctions. Though the spectrum is gapped, the evanescent BdG modes have some real component to their "momenta" and that is what amounts to saying *'multiple back-and-forth reflections'*.

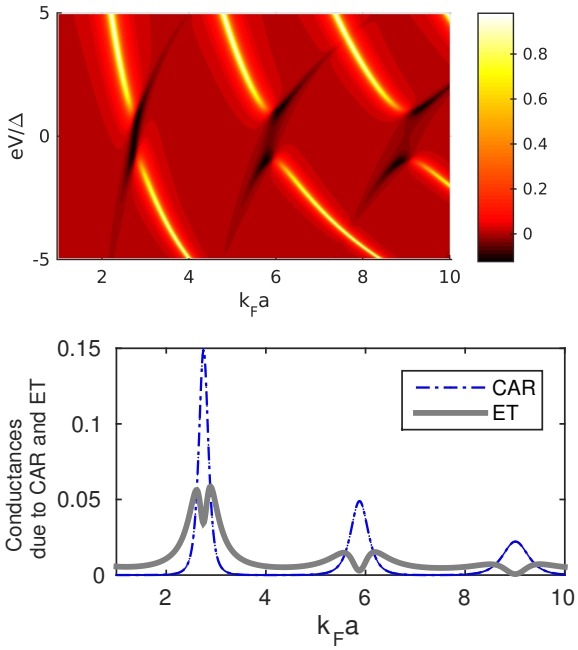

FIG. 3: Our calculation of ET and cAR contributions in a single channel NSN geometry with delta-function barriers of $q_0 = 5k_F$ at the NS junctions. G_{RL} is plotted in the upper panel as a contour-plot in units of $2e^2/h$. In the lower panel, ET and cAR contributions to G_{RL} are plotted at a fixed bias $eV = 0\Delta$ as a function of length of the SC region in units of k_F^{-1}. cAR enhancement is π periodic in k_Fa.

When we turn to the experiments, we find that the enhancement factor is even smaller. Russo et al [2] have performed experiments on a set-up that is qualitatively an NM-SC-NM junction with barriers. But, this differs

from the calculations mainly with the fact that the NM's are diffusive and the calculations on ballistic NM-SC-NM cannot be taken very seriously. However, enhancement of cAR is signalled in experiments and the negative non-local voltage measured is of the order of 10^{-2} times the value of normal state voltage. This has to be contrasted with the value of 0.8 that we get in our calculations. The BdG modes also have an imaginary part to the momentum in addition to the real part which suppresses the non-local subgap transport when the length of the SC is very large. In the opposite limit of a short SC region, the electron to hole conversion is too small. Also, in the limit when barrier strength q_0 is much smaller than the Fermi wavenumber k_F, the effect of barrier becomes negligible and the dominance of ET is restored. Ideally, to enhance cAR in this setup, $k_F a \sim \pi$ and $q_0 \gtrsim k_F$, so that there is some scope for few back-and-forth reflections for the BdG quasiparticle modes before they decay (real part of k is responsible for this interference) and the electron to hole conversion will also happen.

Josephson junction between two-dimensional superconductors

A system closely related to the ladder proposed here is a Josephson junction between two two-dimensional superconductors. The Hamiltonian that describes such a Josephson junction is:

$$\begin{aligned} H &= \sum_s \Bigg[\Psi_s^\dagger(x,y) \Big\{ -\Big(\frac{\hbar^2}{2m}\frac{\partial^2}{\partial x^2} + \frac{\hbar^2}{2m}\frac{\partial^2}{\partial y^2} + \mu\Big)\tau_z \\ &\quad + \Delta \left[\cos[\phi(y)]\ \tau_x + \sin[\phi(y)]\ \tau_y\right] \Big\} \Psi_s(x,y) \Bigg], \\ &\quad \text{where} \quad \phi(y) = 0 \quad \text{for} \quad y > 0, \\ &\quad \text{and} \quad \phi(y) = -\phi \quad \text{for} \quad y < 0. \end{aligned} \tag{8}$$

The dispersion in the bulk for this Hamiltonian is

$$E(\vec{k}) = \pm\sqrt{(\hbar^2\vec{k}^2/2m - \mu)^2 + \Delta^2}, \tag{9}$$

and the bulk gap is 2Δ. We will show that a non-zero ϕ can induce one-dimensional states localised at the junction. BC for the junction is- $\psi(x, y = 0^+) = \psi(x, y = 0^-)$ and $[\partial_y\psi(x,y)|_{y=0^+} - \partial_y\psi(x,y)|_{y=0^-}] = q_0\psi(x, y = 0)$. The parameter q_0 characterises the transparency of the junction. The limits $q_0 = 0$ and $q_0 \to \infty$ correspond to fully transperent and fully opaque junctions respectively. The subgap states need to have at least one out of k_x and k_y to be complex. Since the junction is in y-direction, k_y will be complex. Translational invariance of the system along x-direction makes k_x a good quantum number and real valued. At a given energy E in the gap (i.e., $|E| < \Delta$) and a particular spin eigensector s, the wavefunction will be

$$\psi(x,y) = e^{ik_x x} \cdot \sum_{\nu=\pm} A_{s_y,\nu} e^{i\nu k_R y - s_y \kappa y}\ \vec{u}_{s_y,\nu}, \tag{10}$$

where $k_y = \nu k_R + i s_y \kappa$, $(k_R,\ \kappa > 0)$, $\vec{k} = (k_x, k_y)$, $\vec{k}$ is related to E by the dispersion relation eq. (9), $s_y = sign(y)$, and $\vec{u}_{s_y,\nu}$ is the eigen-spinor that is a function of $k_y = \nu k_R + i s_y \kappa$. Now, substituting the above wavefunction in the BC implies that a subgap state exists if and only if $\mathrm{Det}[M] = 0$, where M is 4×4 matrix, given by:

$$\begin{aligned} M &= \begin{bmatrix} M_1 & M_2 \end{bmatrix}, \text{ where} \\ M_1 &= \begin{bmatrix} \vec{u}_{+,+} & \vec{u}_{+,-} \\ (ik_{+,+} - q_0)\vec{u}_{+,+} & (ik_{+,-} - q_0)\vec{u}_{+,-} \end{bmatrix} \\ M_2 &= \begin{bmatrix} \vec{u}_{-,+} & \vec{u}_{-,-} \\ -ik_{-,+}\ \vec{u}_{-,+} & -ik_{-,-}\ \vec{u}_{-,-} \end{bmatrix}. \end{aligned} \tag{11}$$

We numerically show in the Fig. 4 that a nonzero phase

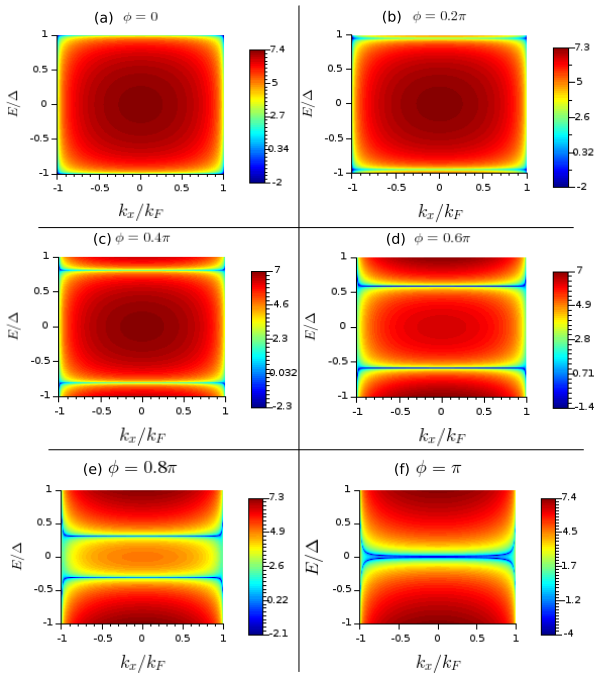

FIG. 4: $\log|\mathrm{Det.}[M]|$ plotted as a function of E and k_x for various choices of ϕ. Dark blue regions in each contour plot indictae the existence of subgap states localised along the junction. We have chosen $q_0 = 0$ everywhere.

difference ϕ results in subgap states, that go deeper into the gap as ϕ approaches π. The dispersion of the 1D modes is almost flat in the middle, while for k_x near $\pm k_F$, the dispersion has a sharp slope and connects to energies $\pm\Delta$ smoothly.

Transport in a layered superconductor with a phase difference

Here, we explain the transport calculation for the system where two two dimensional normal metals are attached to a layered two-dimensional superconductor where two layers have different SC phases. This is a generalisation of the ladder system to two-dimensions. The Hamiltonian for the layer region ($0 \leq x \leq a$) can be written as:

$$\begin{aligned} H \;=\; \sum_{\lambda,s} \Bigg[& \Psi^{\dagger}_{s,\lambda}(\vec{r}) \Big\{ \Big[\frac{-\hbar^2}{2m} \Big(\frac{\partial^2}{\partial x^2} + \frac{\partial^2}{\partial y^2} \Big) - \mu \Big] \tau_z \\ & + \Delta(\cos\phi_\lambda \tau_x \quad + \sin\phi_\lambda \tau_y) \Big\} \Psi_{s,\lambda}(x) \\ & + g \; \Psi^{\dagger}_{s,\lambda}(x) \tau_z \Psi_{s,\bar{\lambda}}(\vec{r}) \Bigg], \end{aligned} \tag{12}$$

where (i) $s = \uparrow, \downarrow$ and $\lambda = 1, 2$ are spin and wire indices respectively, (ii) $\bar{s}/\bar{\lambda}$ takes the value of the label index different from s/λ, and (iii) $\Psi_{s,\lambda}(\vec{r}) = [\sigma_s c_{s,\lambda}(\vec{r}),\ d_{s,\lambda}(\vec{r})]^T$, where $\sigma_{\uparrow/\downarrow} = \pm 1$. The Hamiltonians for the NM regions on the left ($x < 0$) and right ($x > a$) are given by $H = \sum_s c^{\dagger}_s(\vec{r})[\hbar^2\vec{k}^2/2m - \mu]c_s(\vec{r})$. Here onwards, we shall leave out the spin index s. A factor of 2 to account for spin degeneracy will multiply the conductances in the final result. The SC phases ϕ_λ on the two layers ($\lambda = 1, 2$) can be chosen to be $\phi_1 = 0$, and $\phi_2 = -\phi$, without loss of generality so that $(\phi_1 - \phi_2) = \phi$.

It can be seen from here that the system is transnationally invariant along $\vec{y}$-direction. Hence k_y is a good quantum number. For a given value of k_y, the problem becomes effectively one dimensional. The discussion in the section "*Calculation*" of the main paper (from eq.(1) until except eq.(5)) holds good with the change: $\mu \rightarrow (\mu - \hbar^2 k_y^2/2m)$. To get the final expression for transconductance from scattering amplitudes, an integral over all possible angles of incidence at a given energy must be performed (spanning different values of k_y as will be discussed further). Let $\vec{k} = (k_x, k_y) = k(\cos\theta, \sin\theta)$. Then, the differential transconductance per unit length of cross-section is given by:

$$\begin{aligned} & G_{RL}(V) \\ & = \frac{2e^2}{h} \Big[\int_{-\pi/2}^{\pi/2} d\theta \cos\theta \; |t_n(eV,\theta)|^2 \\ & - \int_{-\theta_c}^{\theta_c} d\theta \cos\theta_h \; \sqrt{(\mu - eV)/(\mu + eV)} \; |t_a(eV,\theta)|^2 \Big], \end{aligned}$$

where $\theta_c = \sin^{-1}[(\mu - eV)/(\mu + eV)]$ if $V > 0$, while $\theta_c = \pi/2$ if $V \leq 0$ and $\theta_h = \sin^{-1}[\sin\theta\,(\mu + eV)/(\mu - eV)]$. Here, θ is the angle at which incident electron hits the NM-SC layer interface, with $\theta = 0$ corresponding to the normal incidence and $\theta = \pm\pi/2$ corresponding to glancing angle. θ_c is the critical angle beyond which the transmitted hole on the other NM is evanescent mode (this happens because the Fermi surfaces at energies $+eV$ and $-eV$ with respect to the Fermi energy have different lengths). We calculated the differential transconductance using this formula and the results can be seen in Fig. 5. It

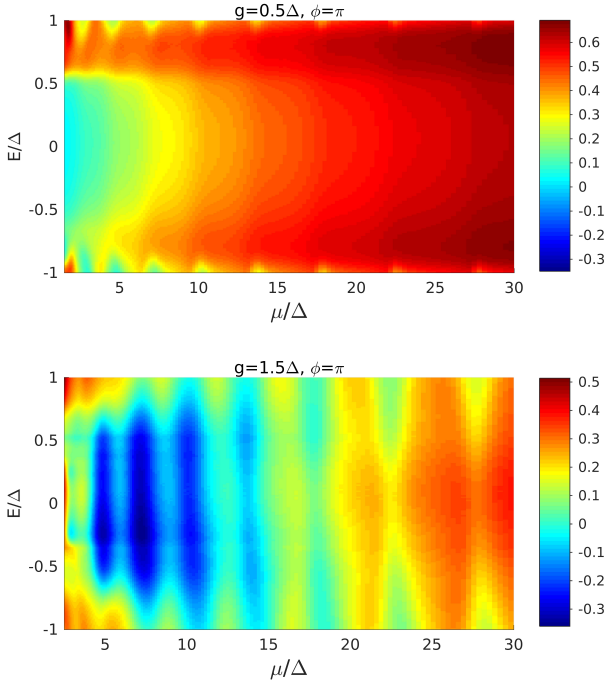

FIG. 5: Differential transconductance per unit length of cross-section in a 2d analogue of the ladder system in units of $2e^2/h$. Parameters: $m = 1.0,\ a = 6\hbar/\sqrt{2m\Delta},\ \phi = \pi$.

can be seen from the contour plots of G_{RL} versus (μ, E) that the features of Fabry-Pérot type interference continue to persist even in the two-dimensional setup though the values of enhanced cAR ($G_{RL} \;-0.35\; 2e^2/h$) may not be as high as in the one-dimensional ladder model ($G_{RL} \;\sim -0.8\; 2e^2/h$).

[1] N. M. Chtchelkatchev, JETP Lett. 78, 230 - 235 (2003).
[2] S. Russo, M. Kroug, T. M. Klapwijk, and A. F. Morpurgo, Phys. Rev. Lett. 95, 027002 (2005).
[3] G. E. Blonder, M. Tinkham, and T. M. Klapwijk, Phys. Rev. B 25, 4515 (1982).
[4] M. Carreau, E. Farhi, and S. Gutmann, Phys. Rev. D 42, 1194 (1990).
[5] M. Tinkham, Introduction to Superconductivity (McGraw-Hill, New York, 1975), Chapter 6.